We are IntechOpen,
the world's leading publisher of Open Access books
Built by scientists, for scientists

6,900
Open access books available

185,000
International authors and editors

200M
Downloads

154
Countries delivered to

Our authors are among the

TOP 1%
most cited scientists

12.2%
Contributors from top 500 universities

CLARIVATE ANALYTICS
BOOK CITATION INDEX
INDEXED

WEB OF SCIENCE™

Selection of our books indexed in the Book Citation Index
in Web of Science™ Core Collection (BKCI)

Interested in publishing with us?
Contact book.department@intechopen.com

Climate Change:
Is It More Predictable Than We Think?

Rafail V. Abramov
Dept. of Mathematics, Statistics and Computer Science, University of Illinois at Chicago
USA

1. Introduction

The global climate system ties together many physical variables, such as flow velocity, density, pressure, temperature, to name a few. The core equations of the climate system are the primitive evolution equations of the atmosphere and ocean (Lions et al., 1992a;b; 1993a;b; 1995; Majda, 2003), which directly involve the flow velocity (or, alternatively, streamfunction and vorticity), density and pressure. To incorporate the effects of other relevant physical processes which supply the energy to or draw it from the motion of the flow, the primitive equations are coupled to other physical processes through temperature, water vapor, ocean surface pressure, and other variables. The coupling terms often preserve energy balance, that is, at any moment, the sum of energy transfer rates between all coupled processes is zero.

The main difficulty in the study of the behavior of primitive equations lies in the nonlinearity of the dynamics of velocity or streamfunction-vorticity in the advection term. The nonlinearity of the primitive equations is also the main source of chaos and lack of predictability for long times in the weather and climate prediction. As has first been recognized by Lorenz (1963), even a simple three-variable nonlinear dynamical system (the so-called Lorenz attractor), based on the idealized convection cell with cooling at the top and heating at the bottom, exhibits extreme sensitivity to initial conditions. Nowadays, the Lorenz attractor is considered a canonical textbook example of chaos in a nonlinear dynamical system, with many illustrations depicting two nearly identical initial conditions evolving into two unrelated trajectories after a short period of time. In more complex dynamical systems with advection terms, nonlinear chaos develops in much more sophisticated fashion, making long-term forecasts difficult and uncertain.

Despite nonlinearity and chaos in the dynamics of the atmosphere and oceans, it has long been recognized by scientists that that the observed motion of the flow can be decomposed into a multitude of different spatio-temporal scales, ranging from thousands of kilometers and many years to few hundred meters and several minutes. The slowest-varying modes, constituting low frequency variability (LFV), involve large scale spatial patterns, usually called "oscillations". The examples of these patterns are the well-known El Niño Southern Oscillation (ENSO), Arctic Oscillation (AO), Antarctic Oscillation (AAO), and North Atlantic Oscillation (NAO). The rest of the spatio-temporal scales constitute much faster fluctuations, superimposed with the slowly varying LFV modes. It is believed by a number of scientists that the mutual combination of the states of LFV modes plays a major role in the present planetary climate (Crowley, 2000; Delworth & Knutson, 2000), and, therefore, the projection

of behavior of LFV modes into the future is one of the key considerations for the climate change prediction.

One of the interesting questions about the dynamics of low frequency variability is the effect of its coupling with the faster small scale processes on nonlinear chaotic behavior of LFV modes. Does short time scale chaos and rapid mixing make the long time behavior of LFV modes more chaotic, or otherwise? The nonlinear variables of the low frequency variability, as well as small scale fast processes, are the velocity/streamfunction fields, due to nonlinear advection terms of the primitive equations. In these variables, the energy emerges as a positive-definite quadratic form, and, therefore, the direct coupling between velocity/streamfunction fields of LFV and fast dynamics should preserve such a form to reflect the energy balance during its transfer between the large scale slow motion and fast small scale processes. In Section 2 of this chapter, we present the results of the recent study (Abramov, 2011c) how the fast small scale variables affect chaotic properties of the slow variables through linear energy-preserving coupling in a general nonlinear two-scale model with quadratic energy. White linear coupling is the simplest form of coupling between slow and fast variables, it is nonetheless common in interactions between velocity/streamfunction variables (see, for example, the model of mean flow – small scale interactions via topographic stress in Grote et al. (1999), where the total energy conservation in the coupling between the zonal mean flow and small scale fluctuations is a key requirement). For the simple two-scale Lorenz 96 model (Abramov, 2010; Fatkullin & Vanden-Eijnden, 2004; Lorenz, 1996; Lorenz & Emanuel, 1998), which mimics certain large-scale features of the atmosphere such as the Rossby waves, we show through numerical simulations that chaos at slow variables can be suppressed by the rapidly mixing fast variables, even to the point when the behavior of the slow variables becomes completely predictable.

Another interesting question arises immediately from the first one. Often, it is not possible to model a large multiscale dynamical system through a direct numerical simulation, due to both the exceedingly large number of fast variables, and the need to use a small time discretization step in the numerical scheme to resolve the motion of the fast variables. In this case, one solution is to make a suitable closure for the slow variables only, using the averaging formalism for the fast variables (Papanicolaou, 1977; Vanden-Eijnden, 2003; Volosov, 1962). However, there is a technical difficulty associated with the averaging formalism: at every given state of the slow variables, one has to know the statistics of the motion of the isolated fast variables with given slow state treated as a parameter. Generally, the statistics of a nonlinear fast dynamics are not known explicitly, and, therefore, either a statistical numerical simulation with the fast variables has to be performed at a each time step of the slow variables, or a suitable approximation for relevant fast statistics has to be constructed. Sometimes, the impact of fast unresolved variables in LFV dynamics is modeled through a constant reference forcing (Abramov & Majda, 2009; Franzke, 2002; Selten, 1995), which does not reflect the response of the statistics of the fast variables to changes in the state of the slow variables. However, the results in Section 2 clearly indicate that chaos at slow variables can be suppressed by the interactions with fast variables. Thus, the question is: how to capture the suppression of chaos at slow variables in a closed model for slow variables only, through a suitable but simple approximation? In Section 3 we demonstrate that an additional linear correction to the reduced equations for the slow dynamics is sufficient to reproduce major statistics of the slow variables in a fully coupled model. This correction emerges from the approximation of the statistical response of the fast variables to changes in slow variables, based on the

linear fluctuation-dissipation theorem (Majda et al., 2005; Risken, 1989). Section 3 is based on Abramov (2011b).

2. Suppression of chaos at slow variables via linear energy-preserving coupling

Dynamical systems, where the evolution of variables is separated between two or more different time scales, are common in the atmospheric/ocean science (Buizza et al., 1999; Franzke et al., 2005; Hasselmann, 1976; Palmer, 2001). The structure of these systems is typically characterized by the existence of a special subset of slow variables, which evolve on a much longer time scale than the rest of the variables. In particular, one can think of the low-frequency variability models in the atmospheric science, where the slow variables, usually the large scale empirical orthogonal functions describing the large-scale slowly-varying patterns in the atmosphere (such as the Arctic or North Atlantic oscillations, for example), are coupled with small-scale fast processes, which are often very chaotic, turbulent and unpredictable (with respect to the slow time scale, that is). One of the key questions about the behavior of multiscale dynamics is the effect of the rapidly mixing turbulent fast dynamics on the chaotic properties of the slow variables.

In this section we present the results of Abramov (2011c), where the chaotic behavior of slow variables is studied by applying the averaging formalism to the dynamics of the linearized model for the slow variables in a two-scale dynamical system with linear energy-preserving coupling. In particular, we consider a two-scale system of autonomous ordinary differential equations of the form

$$\frac{\mathrm{d}\boldsymbol{x}}{\mathrm{d}t} = \boldsymbol{f}(\boldsymbol{x}) + \lambda_y \boldsymbol{L}\boldsymbol{y}, \qquad \frac{\mathrm{d}\boldsymbol{y}}{\mathrm{d}t} = \boldsymbol{g}(\boldsymbol{x}) - \lambda_x \boldsymbol{L}^T \boldsymbol{x}, \qquad (1)$$

where $\boldsymbol{x} = \boldsymbol{x}(t) \in \mathbb{R}^{N_x}$ are the slow variables, $\boldsymbol{y} = \boldsymbol{y}(t) \in \mathbb{R}^{N_y}$ are the fast variables, with $N_y \gg N_x$, $\boldsymbol{f}$ and $\boldsymbol{g}$ are N_x and N_y vector-valued nonlinear functions of $\boldsymbol{x}$ and $\boldsymbol{y}$, respectively, $\boldsymbol{L}$ is a constant $N_x \times N_y$ matrix, and $\lambda_x, \lambda_y > 0$ are the coupling parameters. Here, for simplicity, we assume that $\boldsymbol{L}$ has the full rank, that is, N_x. It can be shown directly that the coupling terms in (1) preserve the quadratic energy of the form

$$E = \lambda_x E_x + \lambda_y E_y, \qquad E_x = \frac{1}{2}\|\boldsymbol{x}\|^2, \qquad E_y = \frac{1}{2}\|\boldsymbol{y}\|^2. \qquad (2)$$

For simplicity of presentation, here we assume that the total energy is a weighted sum of squares of the components of $\boldsymbol{x}$ and $\boldsymbol{y}$; the more general case with energy being an arbitrary positive-definite quadratic form is discussed in Abramov (2011c). Here note that $\boldsymbol{f}(\boldsymbol{x})$ and $\boldsymbol{g}(\boldsymbol{y})$ are not required to preserve the energy, as they might contain forcing and dissipation, which frequently happens in atmosphere/ocean dynamics. For the two-scale system in (1), we look at the averaged dynamics for $\boldsymbol{x}$ alone (Abramov, 2010; Papanicolaou, 1977; Vanden-Eijnden, 2003; Volosov, 1962). The averaging formalism produces the closed system for $\boldsymbol{x}$ in the form

$$\frac{\mathrm{d}\boldsymbol{x}}{\mathrm{d}t} = \boldsymbol{f}(\boldsymbol{x}) + \lambda_y \boldsymbol{L}\bar{\boldsymbol{z}}(\boldsymbol{x}), \qquad (3)$$

where $\bar{\boldsymbol{z}}(\boldsymbol{x})$ is the mean state of the fast variables with $\boldsymbol{x}$ given as a constant parameter:

$$\frac{\mathrm{d}\boldsymbol{z}}{\mathrm{d}t} = \boldsymbol{g}(\boldsymbol{z}) - \lambda_x \boldsymbol{L}^T \boldsymbol{x}, \qquad \bar{\boldsymbol{z}}(\boldsymbol{x}) = \lim_{r \to \infty} \frac{1}{r} \int_0^r \boldsymbol{z}(t)\, \mathrm{d}t. \qquad (4)$$

To observe the chaotic properties of (3), and, in particular, the sensitivity to initial conditions, one has to look at the linearized dynamics of (3), given by

$$\frac{\mathrm{d}\boldsymbol{v}}{\mathrm{d}t} = \left[\frac{\partial \boldsymbol{f}}{\partial \boldsymbol{x}}(\boldsymbol{x}(t)) + \lambda_y \boldsymbol{L}\frac{\partial}{\partial \boldsymbol{x}}\bar{z}(\boldsymbol{x}(t))\right]\boldsymbol{v}, \tag{5}$$

where $\boldsymbol{x}(t)$ is the solution of (3). It is not difficult to see that, for two nearby initial conditions $\boldsymbol{x}_0$ and $\boldsymbol{x}_0^*$ of (3) with $\boldsymbol{v}_0 = \boldsymbol{x}_0^* - \boldsymbol{x}_0$, the solution $\boldsymbol{v}(t)$ of (5) is an approximation of the difference of the trajectories $(\boldsymbol{x}^*(t) - \boldsymbol{x}(t))$, as long as this difference remains small. Then, the sensitivity of (3) to initial conditions is given by the rate of growth of $\|\boldsymbol{v}(t)\|$ in time. For the rate of growth, one can write

$$\frac{1}{2}\frac{\mathrm{d}}{\mathrm{d}t}\|\boldsymbol{v}\|^2 = \boldsymbol{v}^T\frac{\partial \boldsymbol{f}}{\partial \boldsymbol{x}}(\boldsymbol{x}(t))\boldsymbol{v} + \lambda_y \boldsymbol{v}^T\left[\boldsymbol{L}\frac{\partial}{\partial \boldsymbol{x}}\bar{z}(\boldsymbol{x}(t))\right]\boldsymbol{v}. \tag{6}$$

Above, observe that the first term in the right-hand side comes from the uncoupled part of (3), while the second term represents the effect of coupling of the slow variables $\boldsymbol{x}$ to the fast variables $\boldsymbol{y}$. At this point, consider (4), perturbed by a small constant forcing $\delta \boldsymbol{g}$,

$$\frac{\mathrm{d}\boldsymbol{z}}{\mathrm{d}t} = \boldsymbol{g}(\boldsymbol{z}) - \lambda_x \boldsymbol{L}^T\boldsymbol{x} + \delta\boldsymbol{g}, \tag{7}$$

with the perturbed mean state $\bar{z} + \delta\bar{z}$, and denote

$$\boldsymbol{R}(\boldsymbol{x}) = \frac{\delta\bar{z}}{\delta\boldsymbol{g}}. \tag{8}$$

Then, assuming that the small constant perturbation $\delta\boldsymbol{g}$ comes from a small change in $\boldsymbol{x}$, that is,

$$\delta\boldsymbol{g} = -\lambda_x \boldsymbol{L}^T\delta\boldsymbol{x}, \tag{9}$$

for the derivative of $\bar{z}(\boldsymbol{x})$ one obtains, by the chain rule,

$$\frac{\partial}{\partial \boldsymbol{x}}\bar{z}(\boldsymbol{x}) = \frac{\delta\bar{z}}{\delta\boldsymbol{g}}\frac{\partial\delta\boldsymbol{g}}{\partial\delta\boldsymbol{x}} = -\lambda_x\boldsymbol{R}(\boldsymbol{x})\boldsymbol{L}^T. \tag{10}$$

Now, taking into account (10), for (6) we obtain

$$\frac{1}{2}\frac{\mathrm{d}}{\mathrm{d}t}\|\boldsymbol{v}\|^2 = \boldsymbol{v}^T\frac{\partial \boldsymbol{f}}{\partial \boldsymbol{x}}(\boldsymbol{x}(t))\boldsymbol{v} - \lambda_x\lambda_y\boldsymbol{v}^T\boldsymbol{L}\boldsymbol{R}(\boldsymbol{x}(t))\boldsymbol{L}^T\boldsymbol{v}. \tag{11}$$

At this point, one can see that if $\boldsymbol{R}(\boldsymbol{x})$ is positive-definite, then the second term in the right-hand side of (11) becomes negative for arbitrary nonzero $\boldsymbol{v}$, which means that the coupling to the fast variables reduces the rate of growth of $\|\boldsymbol{v}\|$ and decreases chaos in (3), as well as its sensitivity to changes in initial conditions.

When is $\boldsymbol{R}(\boldsymbol{x})$ positive-definite? Generally, since

$$\delta\bar{z} = \boldsymbol{R}(\boldsymbol{x})\delta\boldsymbol{g}, \tag{12}$$

where $\delta\boldsymbol{g}$ is a small constant perturbation in (7), and $\delta\bar{z}$ is the response of the mean state of (7) to $\delta\boldsymbol{g}$, the positive-definiteness of $\boldsymbol{R}(\boldsymbol{x})$ means that

$$\delta\bar{z}^T\delta\boldsymbol{g} = \delta\boldsymbol{g}^T\boldsymbol{R}(\boldsymbol{x})\delta\boldsymbol{g} > 0 \text{ for all sufficiently small } \delta\boldsymbol{g}, \tag{13}$$

that is, the response of the mean state $\delta\bar{z}$ does not develop against the perturbation δg, as long as δg is sufficiently small. It is not difficult to show that the following identity holds whenever δg vanishes:

$$\frac{\mathrm{d}}{\mathrm{d}t}\delta\bar{z} = -\delta g, \tag{14}$$

that is, at the moment the small constant perturbation δg vanishes from (7), the time derivative of $\delta\bar{z}$ equals δg with the opposite sign. Multiplying the above relation by $\delta\bar{z}^T$ on both sides, we obtain

$$\delta\bar{z}^T\frac{\mathrm{d}}{\mathrm{d}t}\delta\bar{z} = \frac{1}{2}\frac{\mathrm{d}}{\mathrm{d}t}\|\delta\bar{z}\|^2 = -\delta\bar{z}^T\delta g < 0, \tag{15}$$

that is, any sufficiently small perturbation of the mean state $\delta\bar{z}$ decreases in time at the moment when the external perturbation δg is removed (stability of mean state under perturbations). An example of such dynamics is the Ornstein-Uhlenbeck process (Uhlenbeck & Ornstein, 1930):

$$\frac{\mathrm{d}z}{\mathrm{d}t} = -\Gamma z + g + \sigma\frac{\mathrm{d}W_t}{\mathrm{d}t} - \lambda_x L^T x, \tag{16}$$

where Γ is a constant positive-definite matrix, g is a constant vector, σ is a constant matrix, and W_t is a Wiener process. Indeed, applying statistical averages on both sides of (16) yields

$$\bar{z} = \Gamma^{-1}(g - \lambda_x L^T x), \tag{17}$$

and, therefore,

$$R = \Gamma^{-1}, \tag{18}$$

which ascertains the positive-definiteness of R. In the case of general nonlinear dynamics in (4), it is shown in Abramov (2011c) that, if the statistical distribution of the solution of (4) can be approximated by the Gaussian probability density with mean state $\bar{z}$ and covariance matrix Σ, then R can be approximated by the integral of the time autocorrelation matrix:

$$R = \left[\int_0^\infty C(s)\,\mathrm{d}s\right]\Sigma^{-1}, \qquad C(s) = \lim_{r\to\infty}\frac{1}{r}\int_0^r z(t+s)(z(t) - \bar{z})^T\,\mathrm{d}t. \tag{19}$$

This is the quasi-Gaussian approximation of $R(x)$ (Abramov, 2009; 2010; 2011a; Abramov & Majda, 2007; 2008; 2009; 2011; Majda et al., 2005). In this case, it is argued in Abramov (2011c) that the positive-definiteness of R must be associated with the situation where the typical Poincaré recurrence time of nonlinear motion around the mean state in (4) (which can be viewed as an advective time scale) is not much shorter than the turbulent mixing autocorrelation time. The reason is that, since $C(0)\Sigma^{-1}$ is the identity matrix, then there always exists $a^* > 0$ such that

$$R_a = \left[\int_0^a C(s)\,\mathrm{d}s\right]\Sigma^{-1} \text{ is positive definite for all } a, \quad 0 < a \le a^*. \tag{20}$$

The positive-definiteness of R_a for larger a can probably be violated by the domination of the rotation part in $C(s)$ for larger s, which evolves on the advective time scale of (4). However, this effect can be prevented by a sufficiently rapid decay of $\|C(s)\|$ for large s, which is governed by the turbulent mixing autocorrelation time. Thus, in general, one can expect the positive-definiteness of R to appear in the situations where the turbulent mixing autocorrelation time scale is not much longer than the advective time scale.

Below we demonstrate through the series of numerical experiments with the two-scale Lorenz 96 model that increasing turbulent mixing at the fast variables promotes positive-definiteness of $\boldsymbol{R}$, as well as decreases chaos at the slow variables.

2.1 The two-scale Lorenz 96 model

The Lorenz 96 model was suggested by Lorenz (1996) as a simple two-scale system which mimics certain large scale features of the atmospheric dynamics, such as Rossby waves. Abramov (2011c) rescaled the Lorenz 96 model using energy rescaling similar to the one used by Majda et al. (2005) for the one-scale Lorenz 96 model. The rescaled model is given by

$$
\begin{aligned}
\dot{x}_i &= x_{i-1}(x_{i+1} - x_{i-2}) + \frac{1}{\beta_x}\left(\bar{x}(x_{i+1} - x_{i-2}) - x_i\right) + \frac{F_x - \bar{x}}{\beta_x^2} - \frac{\lambda_y}{J}\sum_{j=1}^{J} y_{i,j}, \\
\dot{y}_{i,j} &= \frac{1}{\varepsilon}\left[y_{i,j+1}(y_{i,j-1} - y_{i,j+2}) + \frac{1}{\beta_y}\left(\bar{y}(y_{i,j-1} - y_{i,j+2}) - y_{i,j}\right) + \frac{F_y - \bar{y}}{\beta_y^2} + \lambda_x x_i \right],
\end{aligned}
\tag{21}
$$

where $1 \leq i \leq N_x, 1 \leq j \leq J$. Additionally, we write the fast limiting dynamics for (21) as

$$
\dot{z}_{i,j} = z_{i,j+1}(z_{i,j-1} - z_{i,j+2}) + \frac{1}{\beta_y}\left(\bar{z}(z_{i,j-1} - z_{i,j+2}) - z_{i,j}\right) + \frac{F_y - \bar{z}}{\beta_y^2} + \lambda_x x_i,
\tag{22}
$$

where $\boldsymbol{x}$ is given as an external parameter, as in (4). The following notations are adopted above:

- $\boldsymbol{x}$ is the set of the slow variables of size N_x. The following periodic boundary conditions hold for $\boldsymbol{x}$: $x_{i+N_x} = x_i$;
- $\boldsymbol{y}$ is the set of the fast variables of size $N_y = N_x J$ where J is a positive integer. The following boundary conditions hold for $\boldsymbol{y}$: $y_{i+N_x,j} = y_{i,j}$ and $y_{i,j+J} = y_{i+1,j}$;
- F_x and F_y are the constant forcing parameters;
- λ_x and λ_y are the coupling parameters;
- ε is the time scale separation parameter;
- $\bar{x}$ and $\bar{y}$ are the statistical mean states, and β_x and β_y are the statistical standard deviations, respectively, of the corresponding uncoupled dynamics

$$
\begin{aligned}
\frac{\mathrm{d}}{\mathrm{d}t}x_i &= x_{i-1}(x_{i+1} - x_{i-2}) - x_i + F_x, \\
\frac{\mathrm{d}}{\mathrm{d}t}y_{i,j} &= y_{i,j+1}(y_{i,j+1} - x_{i,j+2}) - y_{i,j} + F_y,
\end{aligned}
\tag{23}
$$

separately for slow and fast variables.

In the rescaled Lorenz 96 model (21), F_x and F_y regulate the chaos and mixing of the $\boldsymbol{x}$ and $\boldsymbol{y}$ variables, respectively. However, in the absence of linear rescaling through the mean states $\bar{x}, \bar{y}$, and standard deviations β_x, β_y, the mean state and mean energy would also be affected by the changes in forcing, which affects the mean and energy trends in coupling for the fixed coupling parameters. Thus, the rescaling of the two-scale Lorenz 96 model is needed to adjust the effect of coupling independently of forcing, such that for any F_x and F_y, the mean states and variances of all x_i and $y_{i,j}$ in (21) are approximately zero and one, respectively. At this

point, we can observe that the coupling in the rescaled Lorenz 96 model in (21) preserves the energy

$$E = \lambda_x E_x + \frac{\varepsilon \lambda_y}{J} E_y, \qquad E_x = \frac{1}{2} \sum_{i=1}^{N_x} x_i^2, \qquad E_y = \frac{1}{2} \sum_{i=1}^{N_x} \sum_{j=1}^{J} y_{ij}^2, \tag{24}$$

and the coupling matrix $\boldsymbol{L}$ is given by

$$(\boldsymbol{L}\boldsymbol{y})_i = -\sum_{j=1}^{J} y_{ij}, \qquad (\boldsymbol{L}^T \boldsymbol{x})_{ij} = -x_i. \tag{25}$$

2.2 Suppression of chaos at slow variables by increasing mixing at fast variables

Below, we show the computed statistics of the rescaled Lorenz 96 model (21) with the following parameters: $N_x = 10$, $N_y = 40$, $F_x = 6$, $F_y = 6, 8, 12, 16$ and 24, $\lambda_x = \lambda_y = 0.25$, $\varepsilon = 0.01$ (the time scale separation between $\boldsymbol{x}$ and $\boldsymbol{y}$ is 100 times). The slow forcing parameter $F_x = 6$ is chosen so that the slow dynamics are not too chaotic, mimicking the behavior of low-frequency variability in the atmosphere (it is known from the previous work, such as Abramov (2009; 2010; 2011a); Abramov & Majda (2003; 2007; 2008); Majda et al. (2005) that for $F = 6$ the dynamics of the uncoupled model in (23) are weakly chaotic). The coupling parameters λ_x and λ_y are set to 0.25 so that they are neither too small, nor too large, to ensure rich interaction between the slow and fast variables without linearizing the rescaled Lorenz 96 system too much. The time-scale separation parameter $\varepsilon = 0.01$ is, again, chosen so that it is neither too large, nor too small (the time scale separation by two orders of magnitude is consistent, for instance, with the separation between annual and diurnal cycles in the atmosphere).

In the rescaled Lorenz 96 model (21), it turns out that the values of F_x and F_y do not significantly affect the mean state and mean energy for both the slow variables $\boldsymbol{x}$ and fast variables $\boldsymbol{y}$. To show this, in Table 1 we display the mean states and variances of both $\boldsymbol{x}$ and $\boldsymbol{y}$ for the rescaled Lorenz 96 model in (21). Observe that, despite different forcing regimes, the means and variances for both $\boldsymbol{x}$ and $\boldsymbol{y}$ are almost unchanged, the mean states being near zero while the variances being near one, as designed by the rescaling. Here note that while the rescaling was carried out for the corresponding uncoupled model (where it sets the mean state to zero and variance to one precisely), using the same rescaling parameters in the coupled model (21) still sets its means and variances near prescribed values zero and one, respectively (although not precisely).

At this point, we turn our attention to the chaotic behavior of the slow variables $\boldsymbol{x}$ and mixing behavior of the fast variables $\boldsymbol{y}$ for the same range of parameters. Here we observe the average divergence behavior in time between the short-time (half of the time unit) running averages $\langle \boldsymbol{x} \rangle (t)$ of the slow time series $\boldsymbol{x}(t)$, which are initially generated very closely to each other (for technical details of this simulation, see Abramov (2011c)). The short time-averaging window of half of the time unit for the running average $\langle \boldsymbol{x} \rangle (t)$ ensures that the slow variables $\boldsymbol{x}(t)$ do not change much during this window, while the fast time series $\boldsymbol{y}(t)$ mix completely during the same short time averaging window. The results of this simulation, together with the the time autocorrelation functions for the decoupled fast variables for the same set of parameters with $\boldsymbol{x}$ set to its mean state, are shown in Figure 1. Remarkably, the chaos in the slow $\boldsymbol{x}$-variables is consistently suppressed as the fast forcing F_y increases, as the unperturbed

$N_x = 10$, $N_y = 40$, $F_x = 6$, $\lambda_x = \lambda_y = 0.25$, $\varepsilon = 0.01$				
F_y	x-mean	x-var	y-mean	y-var
6	$9.64 \cdot 10^{-3}$	0.9451	$-2.38 \cdot 10^{-3}$	1.066
8	$2.817 \cdot 10^{-2}$	0.9514	$-1.466 \cdot 10^{-2}$	1.098
12	$2.05 \cdot 10^{-2}$	0.9336	$-2.719 \cdot 10^{-2}$	1.139
16	$-1.353 \cdot 10^{-2}$	0.9006	$-4.028 \cdot 10^{-2}$	1.153
24	$-6.972 \cdot 10^{-2}$	0.8434	$-6.075 \cdot 10^{-2}$	1.167

Table 1. The mean states and variances of the x and y variables for the rescaled Lorenz 96 model in (21) with the following parameters: $N_x = 10$, $N_y = 40$, $F_x = 6$, $F_y = 6, 8, 12, 16$ and 24, $\lambda_x = \lambda_y = 0.25$, $\varepsilon = 0.01$.
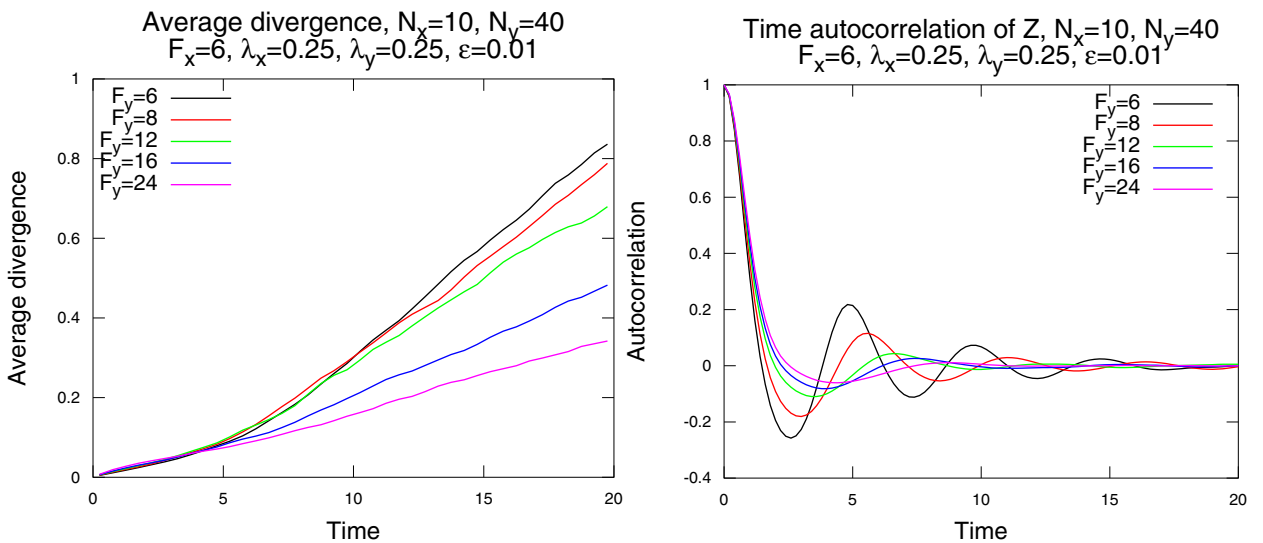
Fig. 1. Left: average divergence between perturbed and unperturbed running averages of the slow variables of (21). Right: the time autocorrelation functions of (22) with x_i fixed at its statistical mean state. The following parameters are used: $N_x = 10$, $N_y = 40$, $F_x = 6$, $F_y = 6, 8, 12, 16$ and 24, $\lambda_x = \lambda_y = 0.25$, $\varepsilon = 0.01$.

and perturbed slow running averages $\langle x \rangle(t)$ diverge from each other slower and slower in time. It cannot be caused by the changing statistical mean or variance of the slow or fast variables creating average counteracting forcing at the slow variables, as Table 1 clearly indicates that the mean states and variances of both the slow and fast variables do not change by a significant amount for different F_y. At the same time, observe that more rapid decay of the time autocorrelation functions for the fast variables is observed as chaos at slow variables is suppressed, supporting the theory developed above and in Abramov (2011c).

In addition, in Figure 2 we demonstrate viability of the quasi-Gaussian approximation to the response $R(x)$ of the mean state $\bar{z}$ in (4) to small constant external forcing, where x is set to the statistical mean state of the slow variables. Observe that as F_y increases and chaos at the slow variables is suppressed, the smallest eigenvalue of the symmetric part of R grows systematically, thus "increasing" positive-definiteness of R. Additionally, the probability density functions of the fast variables are shown in Figure 2 to demonstrate that the statistical distribution of the fast variables is close to Gaussian.
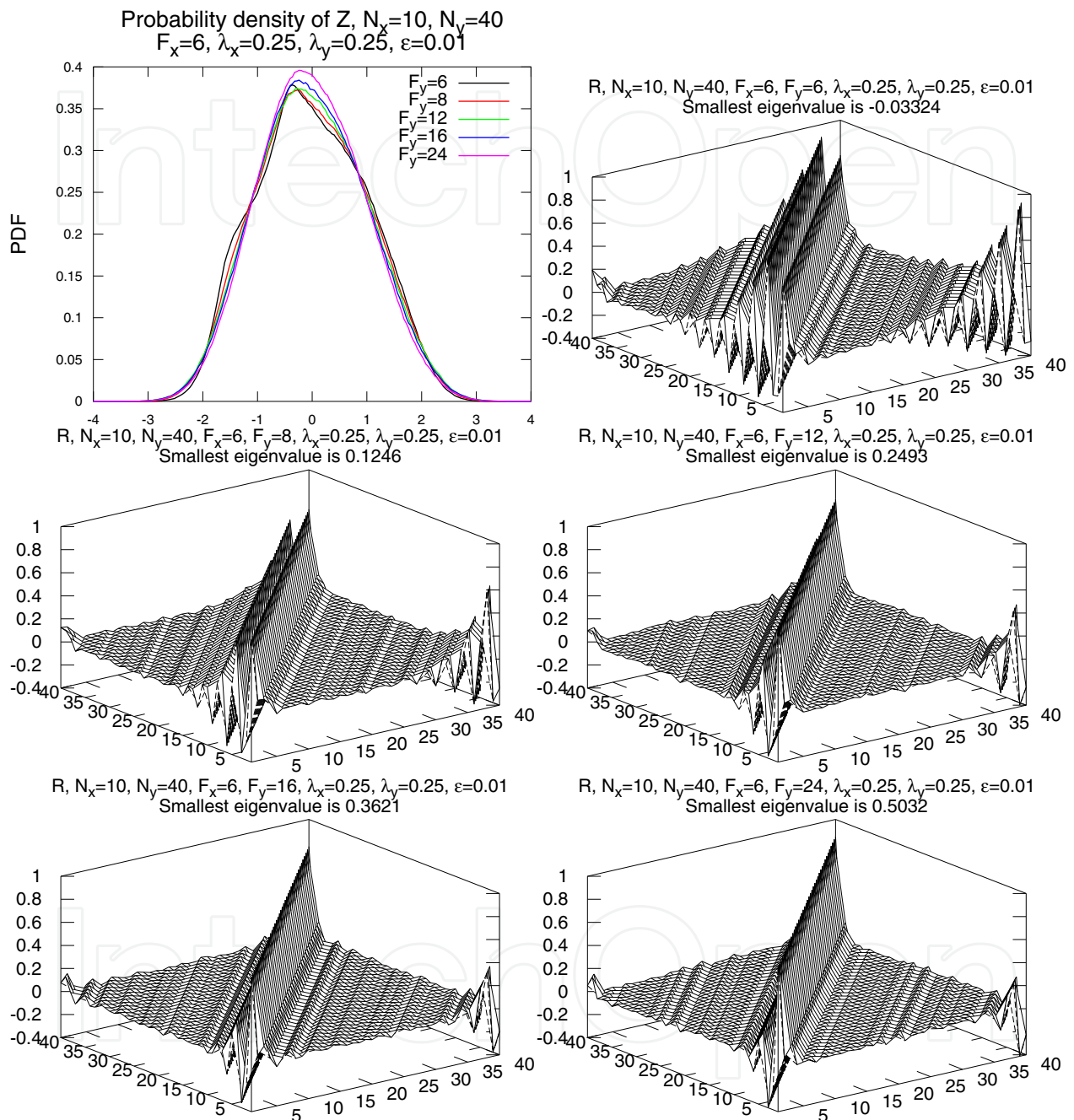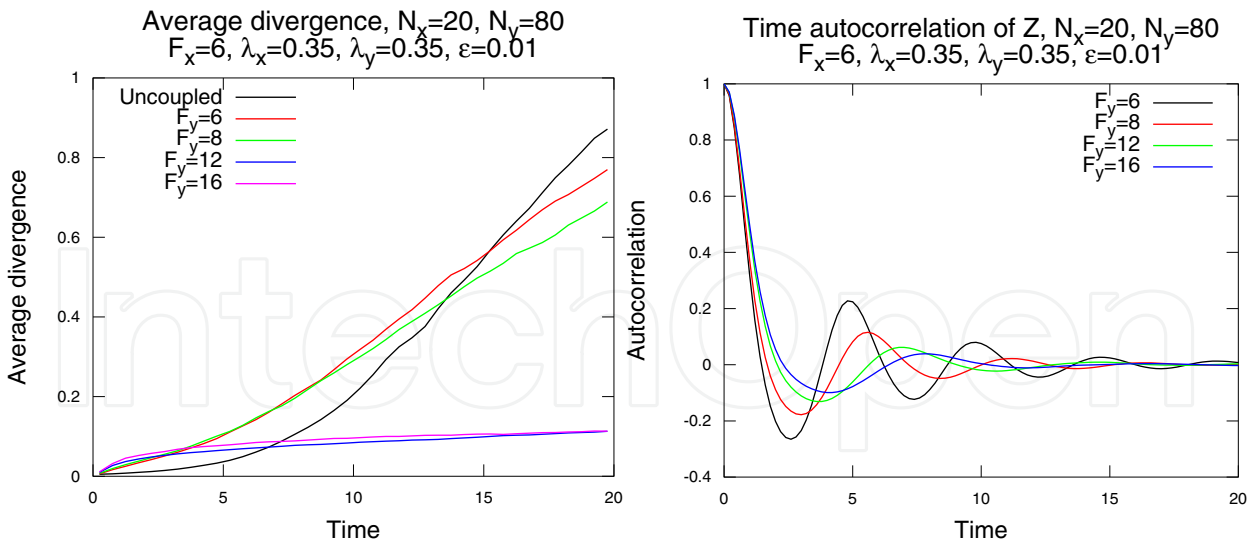
Fig. 2. Upper-left: probability density functions of (22) with x_i fixed at its statistical mean state. The rest: quasi-Gaussian approximations of averaged infinite-time linear response operators $\mathbf{R}(\bar{x})$ for the rescaled Lorenz 96 model in (21) with the following parameters: $N_x = 10$, $N_y = 40$, $F_x = 6$, $F_y = 6, 8, 12, 16$ and 24, $\lambda_x = \lambda_y = 0.25$, $\varepsilon = 0.01$.

Fig. 3. Left: average divergence between perturbed and unperturbed running averages of the slow variables of (21). Right: the time autocorrelation functions of (22) with x_i fixed at its statistical mean state. The following parameters are used: $N_x = 20$, $N_y = 80$, $F_x = 6$, $F_y = 6, 8, 12$ and 16, $\lambda_x = \lambda_y = 0.35$, $\varepsilon = 0.01$, as well as for the uncoupled rescaled Lorenz 96 model with $N = 20$ and $F = 6$.

$N_x = 20, N_y = 80, F_x = 6, \lambda_x = \lambda_y = 0.35, \varepsilon = 0.01$				
F_y	x-mean	x-var	y-mean	y-var
6	$6.216 \cdot 10^{-3}$	0.8878	$-9.982 \cdot 10^{-3}$	1.119
8	$2.34 \cdot 10^{-2}$	0.8728	$-2.791 \cdot 10^{-2}$	1.19
12	-0.1363	0.6927	$-5.553 \cdot 10^{-2}$	1.168
16	-0.1444	0.6703	$-8.669 \cdot 10^{-2}$	1.199

Table 2. The mean states and variances of the x and y variables for the rescaled Lorenz 96 model in (21) with the following parameters: $N_x = 20$, $N_y = 80$, $F_x = 6$, $F_y = 6, 8, 12$ and 16, $\lambda_x = \lambda_y = 0.35$, $\varepsilon = 0.01$.

Another key question in the atmosphere/ocean science is whether the uncoupled system, consisting of slow variables only, is more or less chaotic than its original version, coupled with the fast, often unresolved or underresolved variables. Indeed, often scientists work with uncoupled models consisting of slow variables only, where coupling terms were replaced with the estimates of the long-term averages of the corresponding fast variables, such as the T21 barotropic model with the realistic Earth topography (Abramov & Majda, 2009; Franzke, 2002; Selten, 1995), and study dynamical properties of the slow variables in the uncoupled models. The common sense in this case suggests that if the uncoupled slow model is chaotic, then, naturally, its original version coupled with fast rapidly mixing dynamics should be even more chaotic.

Remarkably, the common sense logic in this situation is deceiving. In fact, it turns out to be possible even to reach the transition from the chaotic to stable slow dynamics by increasing the turbulent mixing at the fast variables, while the uncoupled slow dynamics remain chaotic. Here we demonstrate such an example for the rescaled Lorenz 96 model in (21) with the following set of parameters: $N_x = 20$, $N_y = 80$, $F_x = 6$, $\lambda_x = \lambda_y = 0.35$, $\varepsilon = 0.01$, and compare

it with the uncoupled rescaled Lorenz 96 model with the same parameters $N = 20$ and $F = 6$ for the slow variables. In Figure 3 we show the average divergence of a perturbed trajectory from an unperturbed one for this set of parameters. Observe that, while the slow dynamics for $F_y = 6, 8$ and for uncoupled dynamics with $F = 6$ are clearly chaotic, for $F_y = 12$ and greater values the abrupt transition occurs, where the difference between the perturbed and unperturbed x time series does not grow much beyond 10%. The time autocorrelations of the fast variables for the same set of parameters are also shown in Figure 3, while the statistical mean states and variances for and Table 2. Here, the chaos at slow variables is suppressed purely by the dynamical mechanism uncovered in this work; indeed, the mean state and variance of both the slow and fast variables do not change substantially enough to suppress chaos by creating a counteracting mean forcing term at the slow dynamics to suppress F_x (see Table 2 for confirmation), while the time autocorrelation functions for the fast variables in Figure 3 with x set to the mean state decay faster for larger values of F_y, indicating stronger mixing. The key observation here is that the behavior of the uncoupled model with just the slow variables in the same regime is deceiving – it is clearly chaotic, while the full two-scale model loses chaos at the slow variables in more turbulent regimes of the fast dynamics.

3. Capturing statistics of coupled dynamics via simple closure for slow variables

The time-space scale separation of atmospheric dynamics causes its direct numerical simulation to be computationally expensive, due both to the large number of the fast variables and necessity to choose a small discretization time step in order to resolve the fast components of dynamics. In the climate change prediction the situation is further complicated by the fact that climate is characterized by the long-term statistics of the slow LFV modes, which, under small changes of parameters (such as the solar radiation forcing, greenhouse gas content, etc) change over even longer time scale than the motion of the slow variables themselves. In this situation, where long-term statistics of the slow motion patterns need to be captured, the direct forward time integration of the most comprehensive global circulation models (GCM) is subject to enormous computational expense.

As a more computationally feasible alternative to direct forward time integration of the complete multiscale model, it has long been recognized that, if a closed simplified model for the slow variables alone is available, one could use this closed slow-variable model instead to simulate the statistics of the slow variables. Numerous closure schemes were developed for multiscale dynamical systems (Crommelin & Vanden-Eijnden, 2008; Fatkullin & Vanden-Eijnden, 2004; Majda et al., 1999; 2001; 2002; 2003), which are based on the averaging principle over the fast variables (Papanicolaou, 1977; Vanden-Eijnden, 2003; Volosov, 1962). Some of the methods (such as those in Majda et al. (1999; 2001; 2002; 2003)) replace the fast nonlinear dynamics with suitable stochastic processes (Wilks, 2005) or conditional Markov chains (Crommelin & Vanden-Eijnden, 2008), while others (Fatkullin & Vanden-Eijnden, 2004) provide direct closure by suitable tabulation and curve fitting. Majda et al. (2010) used the stochastic mode reduction method in a nonlinear stochastic model which mimicked the behavior of a GCM. However, it seems that all these approaches require either extensive computations to produce a closed model (for example, the methods in Crommelin & Vanden-Eijnden (2008) and Fatkullin & Vanden-Eijnden (2004) require multiple simulations of fast variables alone with different fixed states of slow variables), or somewhat *ad hoc* determination of closure coefficients by matching areas under the time correlation functions (Majda et al., 1999; 2001; 2002; 2003).

In this section we present a simple method of determining the closed model for slow variables alone, which requires only a single computation of appropriate statistics for the fast dynamics with a certain fixed state of the slow variables, developed in Abramov (2011b). The method is based on the first-order Taylor expansion of the averaged coupling term for the fast variables with respect to the slow variables, which was already computed in Section 2. We show through the computations with the appropriately rescaled two-scale Lorenz 96 96 model (21) that, with simple linear coupling in both slow and fast variables, this method produces quite comparable statistics to what is exhibited by the slow variables of the complete two-scale Lorenz 96 model. The main advantage of the method is its simplicity and easiness of implementation, partly due to the fact that the fast dynamics need not be explicitly known (that is, the fast dynamics can be provided as a "black-box" observations), and the parameters of the closed model for the slow variables are determined from the appropriate statistics of the fast variables for a given fixed state of the slow variables. Additionally, the method can be applied even when the statistics for both the slow and fast variables of the full multiscale model are not available due to computational expense.

For the purpose of this work, here we assume that the computation of (4) is practically feasible only for a single choice of the constant parameter $x = x^*$, where x^* is a suitable point, in the vicinity of which the motion occurs, such as the mean state of the original multiscale dynamics in (1), or a nearby state. A poor man's approach in this case is to compute the approximate average at a single point $x = x^*$, which is a zero order approximation:

$$\bar{z}(x) = \bar{z}(x^*) + O(\|x - x^*\|). \tag{26}$$

Here, one has to compute the time average $\bar{z}$, needed for the averaged dynamics in (3), only once, for the time series of (4) corresponding to $x = x^*$. However, as recently found in Abramov (2011c) and demonstrated above in Section 2, this approximation may fail to capture the chaotic properties of the slow variables in (1), because the coupling term in the averaged linearized dynamics (5) would not be reproduced. Here we propose the following first order correction:

$$
\begin{aligned}
\bar{z}(x) &= \bar{z}(x^*) + \frac{\partial \bar{z}}{\partial x}(x^*)(x - x^*) + O(\|x - x^*\|^2) = \\
&= \bar{z}(x^*) - \lambda_x R(x^*) L^T (x - x^*) + O(\|x - x^*\|^2),
\end{aligned}
\tag{27}
$$

where the derivative of $\bar{z}$ with respect to x is already computed in (10) through the linear response R of the statistical mean state to small constant external forcing. The first-order approximation above, applied to (3), leads to the following closed system for the slow variables alone:

$$\frac{dx}{dt} = f(x) + \lambda_y L \bar{z}^* - \lambda_x \lambda_y L R^* L^T (x - x^*), \tag{28}$$

where $\bar{z}^* = \bar{z}(x^*)$ is the time-average of the trajectory in (4) for $x = x^*$, while $R^* = R(x^*)$ is given by (19) for the same value of $x = x^*$.

Even with the linear coupling, the function $\bar{z}(x)$ (the dependence of the mean state of (4) on x) is not generally linear. Thus, the validity of the linear approximation in (28) depends on the influence (or lack thereof) of the nonlinearity of the function $\bar{z}(x)$. While rigorous estimates of the validity of the linear approximation in (28) can hardly be provided in general case, here, instead, we try to justify it by comparing the fast limiting system in (4) to the

Ornstein-Uhlenbeck process in (16). It is easy to see, by applying statistical averages on both sides, that the difference between the statistical mean states of (16) corresponding to x and x^* is

$$\bar{z}_{OU} - \bar{z}_{OU}^* = \Gamma^{-1} L_x (x - x^*), \tag{29}$$

which is valid for $(x - x^*)$ of an arbitrary norm. At the same time, it was already shown in (18) (Section 2) that $R = \Gamma^{-1}$, which means that, in the case of the Ornstein-Uhlenbeck process, the relation (27) is exact for an arbitrarily large perturbation $(x - x^*)$. Hence, if the nonlinear process in (4) behaves statistically similarly to the Ornstein-Uhlenbeck process in (16), the averaged system in (28) can be expected to behave statistically similarly to the slow part of (1). Below we numerically test the approximation for slow variables with linear coupling using the two-scale Lorenz 96 model, the same that was used in Section 2.

3.1 Direct numerical simulation

Here we present a numerical study of the proposed approximation for the slow dynamics, applied to the two-scale Lorenz 96 model in (21). We compare the statistical properties of the slow variables for the three following systems:

1. The complete two-scale Lorenz 96 system from (21);
2. The approximation for the slow dynamics alone from (28);
3. The poor man's version of (28) with the first-order correction term R^* set to zero (further referred to as the "zero-order" system).

The fixed parameter x^* for the computation of R^* was set to the long-term mean state $\bar{x}$ of (21) (in practical situations, a rough estimate could be used).

Due to translational invariance of the studied models, the statistics are invariant with respect to the index shift for the variables x_i. For diagnostics, we monitor the following long-term statistical quantities of x_i:

a. The probability density functions (PDF), computed by bin-counting. A PDF gives the most complete information about the one-point statistics of x_i, as it shows the statistical distribution of x_i in the phase space.
b. The time autocorrelation functions $\langle x_i(t) x_i(t+s) \rangle$, where the time average is over t, normalized by the variance $\langle x_i^2 \rangle$ (so that it always starts with 1).

The success (or failure) of the proposed approximation of the slow dynamics depends on several factors. First, as the quasi-Gaussian linear response formula (19) is used for the computation of R^*, the precision will be affected by the non-Gaussianity of the fast dynamics. Second, it depends how linearly the mean state $\bar{z}$ for the fast variables depends on the slow variables x. Here we observe the limitations of the proposed approximation by studying a variety of dynamical regimes of the rescaled Lorenz 96 model in (21):

- $N_x = 20$, $J = 4$ (so that $N_y = 80$). Thus, the number of the fast variables is four times greater than the number of the slow variables.
- $\lambda_x = \lambda_y = 0.3, 0.4$. These values of coupling are chosen so that they are neither too weak, nor too strong (although 0.3 is weaker, and 0.4 is stronger). Recall that the standard deviations of both x_i and $y_{i,j}$ variables are approximately 1, and, thus, the contribution to the right-hand side from coupled variables is weaker than the self-contribution, but still of the same order.
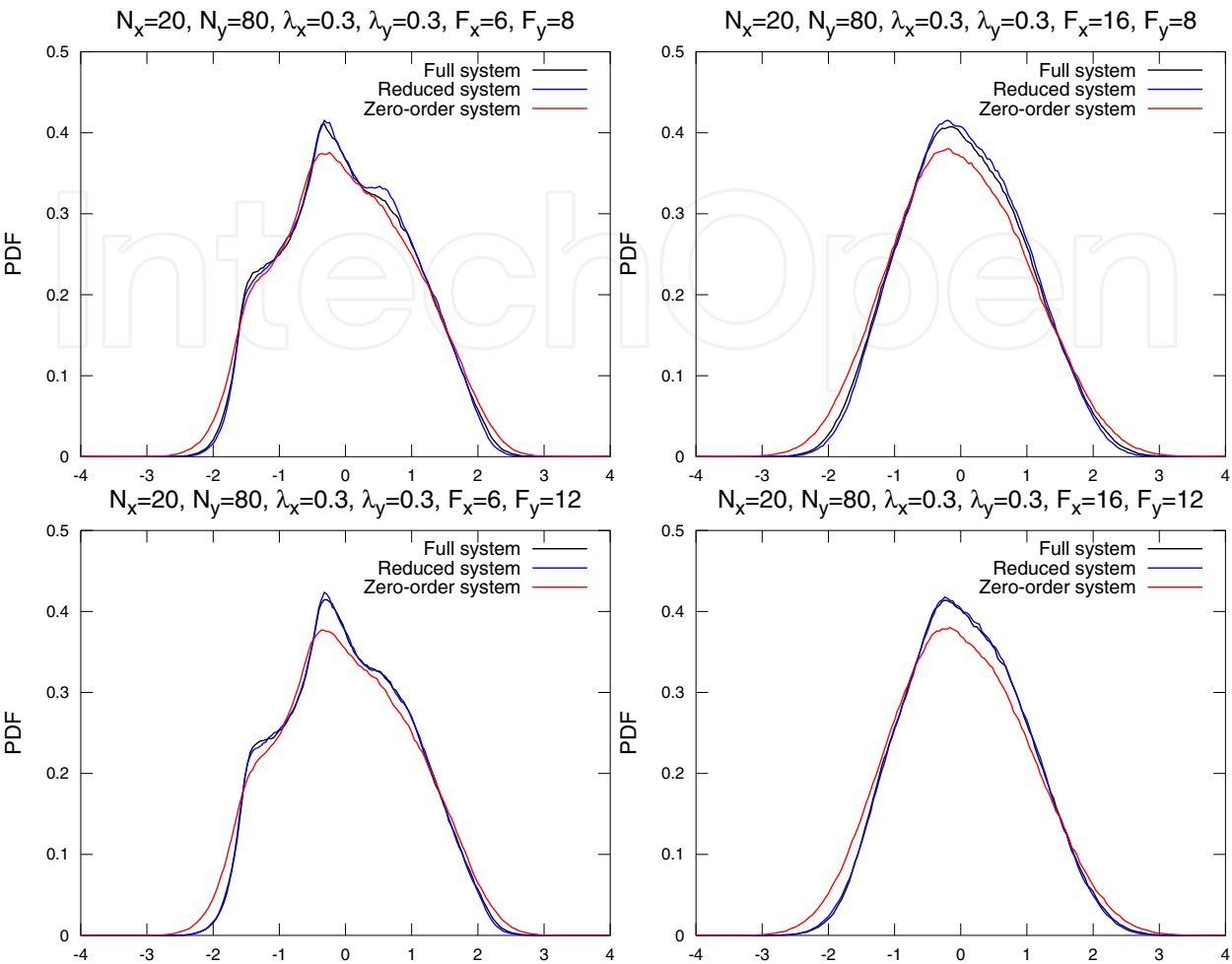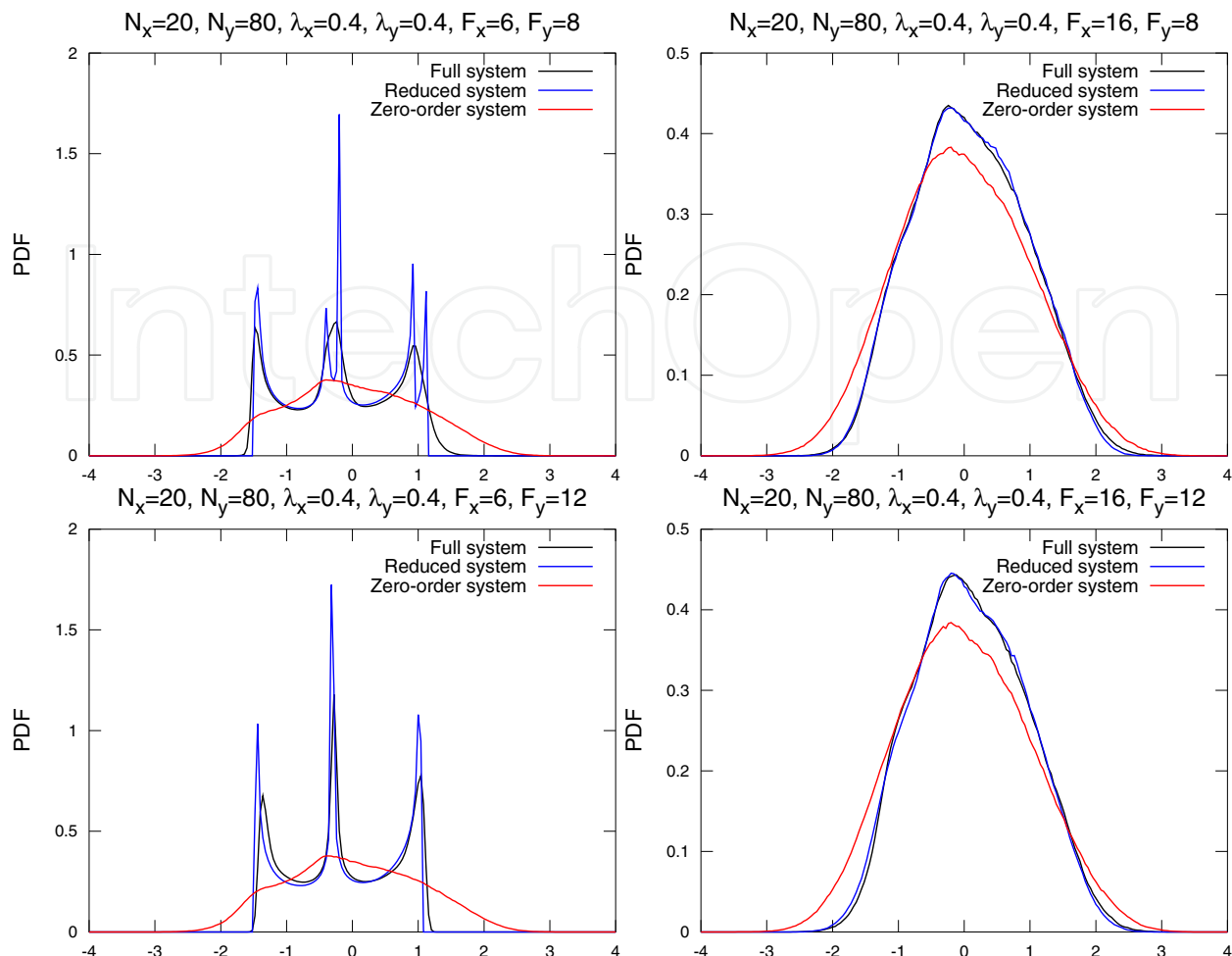
Fig. 4. Probability density functions of the slow variables. The following parameters are used: $N_x = 20$, $N_y = 80$, $F_x = 6, 16$, $F_y = 8, 12$, $\lambda_x = \lambda_y = 0.3$, $\varepsilon = 0.01$.

$\lambda_{x,y} = 0.3$, $F_y = 8$				$\lambda_{x,y} = 0.3$, $F_y = 12$		
	Red.	Z.O.			Red.	Z.O.
$F_x = 6$	$5.036 \cdot 10^{-3}$	$1.165 \cdot 10^{-2}$	$F_x = 6$		$2.581 \cdot 10^{-3}$	$1.576 \cdot 10^{-2}$
$F_x = 16$	$5.593 \cdot 10^{-3}$	$1.469 \cdot 10^{-2}$	$F_x = 16$		$2.71 \cdot 10^{-3}$	$1.818 \cdot 10^{-2}$
$\lambda_{x,y} = 0.4$, $F_y = 8$				$\lambda_{x,y} = 0.4$, $F_y = 12$		
	Red.	Z.O.			Red.	Z.O.
$F_x = 6$	0.1022	$8.857 \cdot 10^{-2}$	$F_x = 6$		$9.28 \cdot 10^{-2}$	0.1113
$F_x = 16$	$3.725 \cdot 10^{-3}$	$2.703 \cdot 10^{-2}$	$F_x = 16$		$5.885 \cdot 10^{-3}$	$3.209 \cdot 10^{-2}$

Table 3. L_2-errors between the PDFs of the slow variables of the full two-scale Lorenz 96 model and the two reduced models. Notations: "Red." stands for "Reduced" (that is, (28)), and "Z.O." stands for "Zero-order", the poor man's version of (28).

Fig. 5. Probability density functions of the slow variables. The following parameters are used: $N_x = 20$, $N_y = 80$, $F_x = 6, 16$, $F_y = 8, 12$, $\lambda_x = \lambda_y = 0.4$, $\varepsilon = 0.01$.

- $F_x = 6, 16$. The slow forcing F_x adjusts the chaos and mixing properties of the slow variables, and in this work it is set to a weakly chaotic regime $F_x = 6$, and strongly chaotic regime $F_x = 16$.
- $F_y = 8, 12$. The fast forcing adjusts the chaos and mixing properties of the fast variables. Here the value of F_y is chosen so that the fast variables are either moderately chaotic for $F_y = 8$, or more strongly chaotic for $F_y = 12$.
- $\varepsilon = 0.01$. The time scale separation of two orders of magnitude is consistent with typical real-world geophysical processes (for example, the annual and diurnal cycles of the Earth's atmosphere).

In Figures 4 and 5 we show the probability density functions of the slow dynamics for the full two-scale Lorenz 96 model, the reduced closed model for the slow variables alone in (28), and its poor man's zero order version without the linear correction term. In addition, in Table 3 we show the L_2-errors in PDFs between the full two-scale Lorenz 96 model and the two reduced models. Observe that for the more weakly coupled regimes with $\lambda_x = \lambda_y = 0.3$ all PDFs look similar, however, the reduced model with the correction term reproduces the PDFs much closer to those of the full two-scale Lorenz 96 model, than the zero-order model. In the more strongly coupled regime with $\lambda_x = \lambda_y = 0.4$ the situation tilts even more in favor of the reduced model with linear correction term in (28): observe that for the weakly chaotic
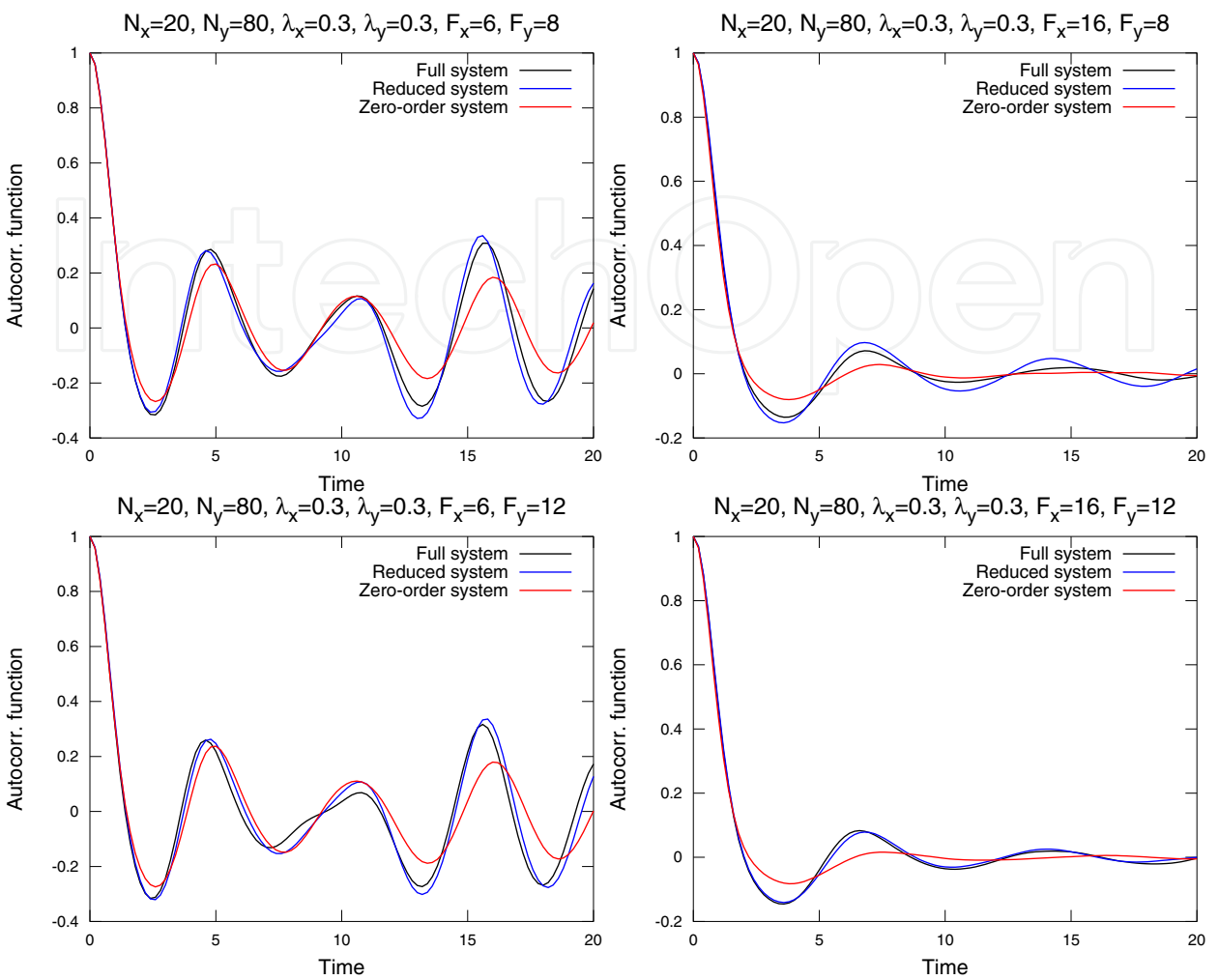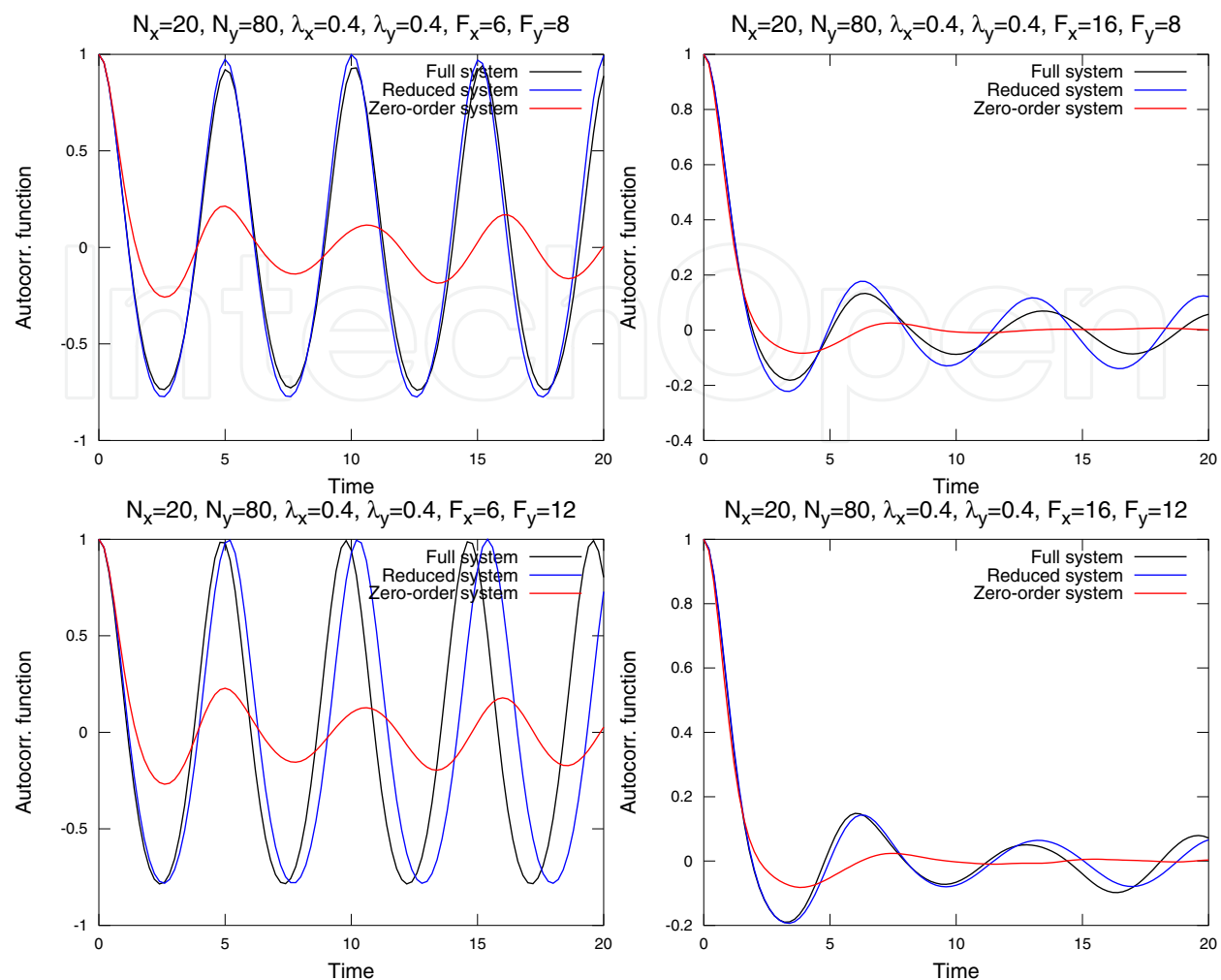
Fig. 6. Time autocorrelation functions of the slow variables. The following parameters are used: $N_x = 20$, $N_y = 80$, $F_x = 6, 16$, $F_y = 8, 12$, $\lambda_x = \lambda_y = 0.3$, $\varepsilon = 0.01$.

$\lambda_{x,y} = 0.3, F_y = 8$			$\lambda_{x,y} = 0.3, F_y = 12$		
	Av.	Z.O.		Av.	Z.O.
$F_x = 6$	$5.841 \cdot 10^{-2}$	0.1211	$F_x = 6$	$6.539 \cdot 10^{-2}$	0.1572
$F_x = 16$	$4.079 \cdot 10^{-2}$	$5.342 \cdot 10^{-2}$	$F_x = 16$	$1.559 \cdot 10^{-2}$	$7.396 \cdot 10^{-2}$
$\lambda_{x,y} = 0.4, F_y = 8$			$\lambda_{x,y} = 0.4, F_y = 12$		
	Av.	Z.O.		Av.	Z.O.
$F_x = 6$	$5.538 \cdot 10^{-2}$	0.3677	$F_x = 6$	0.2981	0.3986
$F_x = 16$	$8.534 \cdot 10^{-2}$	0.1355	$F_x = 16$	$4.835 \cdot 10^{-2}$	0.1482

Table 4. L_2-errors between the time autocorrelation functions of the slow variables of the full two-scale Lorenz 96 model and the two reduced models. Notations: "Red." stands for "Reduced" (that is, (28)), and "Z.O." stands for "Zero-order", the poor man's version of (28).

Fig. 7. Time autocorrelation functions of the slow variables. The following parameters are used: $N_x = 20$, $N_y = 80$, $F_x = 6, 16$, $F_y = 8, 12$, $\lambda_x = \lambda_y = 0.4$, $\varepsilon = 0.01$.

regime with $F_x = 6$ the PDFs of the full two-scale Lorenz 96 model have three sharp peaks, indicating strong non-Gaussianity. The reduced model in (28) reproduces these peaks, while its zero-order version fails. In Figures 6 and 7 we show the time autocorrelation functions of the slow dynamics for the full two-scale Lorenz 96 model, the reduced closed model for the slow variables alone in (28), and its poor man's zero order version without the linear correction term. Just as the PDFs, for the more weakly coupled regimes with $\lambda_x = \lambda_y = 0.3$ the time autocorrelation functions look similar, yet the reduced model with the correction term reproduces the time autocorrelation functions more precisely than the zero-order model. In the more strongly coupled regime with $\lambda_x = \lambda_y = 0.4$ the difference between the reduced model in (28) and its poor man's zero-order version is even more drastic: observe that for the weakly chaotic regime with $F_x = 6$ the time autocorrelation functions of the full two-scale Lorenz 96 model do not exhibit decay (indicating very weak mixing), and the reduced model in (28) reproduces the autocorrelation functions of the full two-scale Lorenz 96 model rather well, while its zero-order version fails. In addition, in Table 4 we show the L_2-errors in time autocorrelation functions (for the correlation time interval of 20 time units, as in Figures 6 and 7) between the full two-scale Lorenz 96 model and the two reduced models. Observe

that, generally, the reduced system in (28) produces more precise results than its poor man's version without the correction term.

4. Conclusions

In this work we made an initial attempt to estimate and reproduce the chaotic properties of a nonlinear multiscale system with linear energy-preserving coupling which mimics major features of low frequency variability dynamics in real-world climate. In particular, we find that, due to the energy-preserving coupling, the sensitivity to initial conditions of the slow variables can be reduced by rapid mixing strong chaos of the fast variables. In addition, we develop a simple closure scheme for the slow variables alone, which captures major statistics of the full multiscale system. These two studies suggest that the predictability of the low frequency variability in multiscale climate dynamics could in practice be better than what is normally presumed today, and future projections of the low frequency variability modes could be captured by a much simpler reduced model for slow variables alone, which could potentially lead to improved climate change prediction. Below we list the major developments and observations of this work.

- A suitable theory of the effect of the fast rapidly mixing dynamics on the chaos at slow variables is developed by applying the averaging formalism to the linearized dynamics of the system. It is found that the linear energy-preserving coupling creates a systematic damping effect on the chaos at the slow scales when the fast dynamics is rapidly mixing.
- This effect is vividly demonstrated for the two-scale Lorenz 96 model, which is also appropriately rescaled so that the adjustments for the mixing regime at the fast variables do not affect the mean state and variance of both the slow and fast variables. In particular, it is shown through direct numerical simulations that the uncoupled slow dynamics may remain chaotic, while the full coupled system loses chaos and becomes completely predictable at the slow scales as the dynamics at the fast scales become more turbulent.
- With help of the observations above, we develop a simple method of constructing the closed reduced model for slow variables of a multiscale model with linear coupling, which requires only a single computation of the mean state and the time autocorrelation function for the fast dynamics with a fixed state of the slow variables. The method is based on the first-order Taylor expansion of the averaged coupling term for the fast variables with respect to the slow variables, which is computed using the linear fluctuation-dissipation theorem. We demonstrate through the computations with the same rescaled Lorenz 96 model that, with simple linear coupling in both slow and fast variables, the developed reduced model produces quite comparable statistics to what is exhibited by the complete two-scale Lorenz 96 model.

Given the above results, the question of improved predictability of low frequency variability and climate becomes more interesting. Indeed, if the coupling to the fast dynamics makes slow processes less chaotic, then the reduced models with constant parameterizations of interactions with fast dynamics could be more chaotic than the actual physical processes they describe. If one can create reduced climate models which capture the chaos suppression effect with adequate skill, the climate change projections can potentially become less uncertain. In the future, the author intends to develop such reduced climate models for a more realistic Earth-like setting, possibly in collaboration with climate scientists. It remains to be seen whether Earth's climate is more predictable than we tend to think.

5. Acknowledgments

6. References

Abramov, R. (2009). Short-time linear response with reduced-rank tangent map, *Chin. Ann. Math.* 30B(5): 447–462.

Abramov, R. (2010). Approximate linear response for slow variables of deterministic or stochastic dynamics with time scale separation, *J. Comput. Phys.* 229(20): 7739–7746.

Abramov, R. (2011a). Improved linear response for stochastically driven systems, *Front. Math. China*, accepted.

Abramov, R. (2011b). A simple linear response closure approximation for slow dynamics of a multiscale system with linear coupling, *Mult. Mod. Simul.*, accepted.

Abramov, R. (2011c). Suppression of chaos at slow variables by rapidly mixing fast dynamics through linear energy-preserving coupling, *Comm. Math. Sci.*, accepted.

Abramov, R. & Majda, A. (2003). Quantifying uncertainty for non-Gaussian ensembles in complex systems, *SIAM J. Sci. Comp.* 26(2): 411–447.

Abramov, R. & Majda, A. (2007). Blended response algorithms for linear fluctuation-dissipation for complex nonlinear dynamical systems, *Nonlinearity* 20: 2793–2821.

Abramov, R. & Majda, A. (2008). New approximations and tests of linear fluctuation-response for chaotic nonlinear forced-dissipative dynamical systems, *J. Nonlin. Sci.* 18(3): 303–341.

Abramov, R. & Majda, A. (2009). New algorithms for low frequency climate response, *J. Atmos. Sci.* 66: 286–309.

Abramov, R. & Majda, A. (2011). Low frequency climate response of quasigeostrophic wind-driven ocean circulation, *J. Phys. Oceanogr.*, accepted.

Buizza, R., Miller, M. & Palmer, T. (1999). Stochastic representation of model uncertainty in the ECMWF Ensemble Prediction System, *Q. J. R. Meteor. Soc.* 125: 2887–2908.

Crommelin, D. & Vanden-Eijnden, E. (2008). Subgrid scale parameterization with conditional Markov chains, *J. Atmos. Sci.* 65: 2661–2675.

Crowley, T. (2000). Causes of climate change over the past 1000 years, *Science* 289: 270–277.

Delworth, T. & Knutson, T. (2000). Simulation of the early 20th century global warming, *Science* 287: 2246–2250.

Fatkullin, I. & Vanden-Eijnden, E. (2004). A computational strategy for multiscale systems with applications to Lorenz 96 model, *J. Comp. Phys.* 200: 605–638.

Franzke, C. (2002). Dynamics of low-frequency variability: Barotropic mode., *J. Atmos. Sci.* 59: 2909–2897.

Franzke, C., Majda, A. & Vanden-Eijnden, E. (2005). Low-order stochastic model reduction for a realistic barotropic model climate, *J. Atmos. Sci.* 62: 1722–1745.

Grote, M., Majda, A. & Grotta Ragazzo, C. (1999). Dynamic mean flow and small-scale interaction through topographic stress, *J. Nonlin. Sci.* 9: 89–130.

Hasselmann, K. (1976). Stochastic climate models, part I, theory, *Tellus* 28: 473–485.

Lions, J., Temam, R. & Wang, S. (1992a). New formulations of the primitive equations of the atmosphere and applications, *Nonlinearity* 5: 237–288.

Lions, J., Temam, R. & Wang, S. (1992b). On the equations of the large-scale ocean, *Nonlinearity* 5: 1007–1053.

Lions, J., Temam, R. & Wang, S. (1993a). Models of the coupled atmosphere and ocean, *Comp. Mech. Adv.* 1: 5–54.

Lions, J., Temam, R. & Wang, S. (1993b). Numerical analysis of the coupled models of atmosphere and ocean, *Comp. Mech. Adv.* 1: 55–119.

Lions, J., Temam, R. & Wang, S. (1995). Mathematical study of the coupled models of atmosphere and ocean, *Math. Pures Appl.* 74: 105–163.

Lorenz, E. (1963). Deterministic nonperiodic flow, *J. Atmos. Sci.* 20(2): 130–148.

Lorenz, E. (1996). Predictability: A problem partly solved, *Proceedings of the Seminar on Predictability*, ECMWF, Shinfield Park, Reading, England.

Lorenz, E. & Emanuel, K. (1998). Optimal sites for supplementary weather observations, *J. Atmos. Sci.* 55: 399–414.

Majda, A. (2003). *Introduction to PDEs and Waves for the Atmosphere and Ocean*, Vol. 9 of *Courant Lecture Notes*, American Mathematical Society and Courant Institute of Mathematical Sciences.

Majda, A., Abramov, R. & Grote, M. (2005). *Information Theory and Stochastics for Multiscale Nonlinear Systems*, Vol. 25 of *CRM Monograph Series of Centre de Recherches Mathématiques, Université de Montréal*, American Mathematical Society. ISBN 0-8218-3843-1.

Majda, A., Gershgorin, B. & Yuan, Y. (2010). Low frequency response and fluctuation-dissipation theorems: Theory and practice, *J. Atmos. Sci.* 67: 1186–1201.

Majda, A., Timofeyev, I. & Vanden-Eijnden, E. (1999). Models for stochastic climate prediction, *Proc. Natl. Acad. Sci.* 96: 14687–14691.

Majda, A., Timofeyev, I. & Vanden-Eijnden, E. (2001). A mathematical framework for stochastic climate models, *Comm. Pure Appl. Math.* 54: 891–974.

Majda, A., Timofeyev, I. & Vanden-Eijnden, E. (2002). A priori tests of a stochastic mode reduction strategy, *Physica D* 170: 206–252.

Majda, A., Timofeyev, I. & Vanden-Eijnden, E. (2003). Systematic strategies for stochastic mode reduction in climate, *J. Atmos. Sci.* 60: 1705–1722.

Palmer, T. (2001). A nonlinear dynamical perspective on model error: A proposal for nonlocal stochastic-dynamic parameterization in weather and climate prediction models, *Q. J. R. Meteor. Soc.* 127: 279–304.

Papanicolaou, G. (1977). Introduction to the asymptotic analysis of stochastic equations, *in* R. DiPrima (ed.), *Modern modeling of continuum phenomena*, Vol. 16 of *Lectures in Applied Mathematics*, American Mathematical Society.

Risken, H. (1989). *The Fokker-Planck Equation*, 2nd edn, Springer-Verlag, New York.

Selten, F. (1995). An efficient description of the dynamics of barotropic flow, *J. Atmos. Sci.* 52: 915–936.

Uhlenbeck, G. & Ornstein, L. (1930). On the theory of the Brownian motion, *Phys. Rev.* 36: 823–841.

Vanden-Eijnden, E. (2003). Numerical techniques for multiscale dynamical systems with stochastic effects, *Comm. Math. Sci.* 1: 385–391.

Volosov, V. (1962). Averaging in systems of ordinary differential equations, *Russian Math. Surveys* 17: 1–126.

Wilks, D. (2005). Effects of stochastic parameterizations in the Lorenz '96 system, *Q. J. R. Meteorol. Soc.* 131: 389–407.
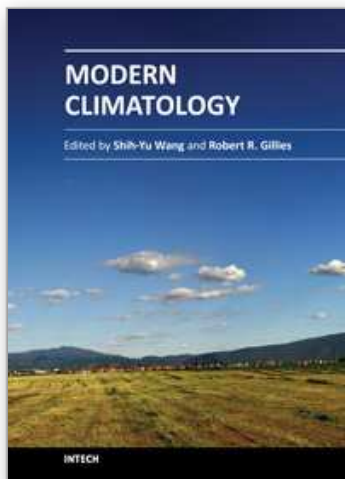
Modern Climatology

Edited by Dr Shih-Yu Wang

Climatology, the study of climate, is no longer regarded as a single discipline that treats climate as something that fluctuates only within the unchanging boundaries described by historical statistics. The field has recognized that climate is something that changes continually under the influence of physical and biological forces and so, cannot be understood in isolation but rather, is one that includes diverse scientific disciplines that play their role in understanding a highly complex coupled "whole system" that is the earth's climate. The modern era of climatology is echoed in this book. On the one hand it offers a broad synoptic perspective but also considers the regional standpoint, as it is this that affects what people need from climatology. Aspects on the topic of climate change - what is often considered a contradiction in terms - is also addressed. It is all too evident these days that what recent work in climatology has revealed carries profound implications for economic and social policy; it is with these in mind that the final chapters consider acumens as to the application of what has been learned to date.

INTECH
open science | open minds